Propulsion and Power Research 2019;8(3):253–262

http://ppr.buaa.edu.cn/

Propulsion and Power Research

www.sciencedirect.com

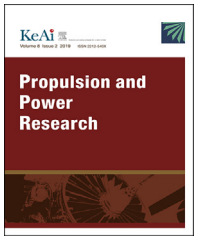

ORGINAL ARTICLE

Peristaltic transport of Herschel-Bulkley fluid in a non-uniform elastic tube

C.K. Selvi, A.N.S. Srinivas*

Department of Mathematics, School of Advanced Sciences, VIT University, Vellore, 632014, Tamilnadu, India

Received 4 December 2017; accepted 22 July 2018
Available online 24 August 2019

KEYWORDS

Peristaltic flow;
Non-uniform tube;
Non-newtonian fluid;
Yield stress;
Volume flow rate;
Elasticity

Abstract The influence of elasticity on peristaltic transport of Herschel-Bulkley fluid in a tube of non-uniform cross-section is investigated. The exact solutions for flow quantities such as velocity, stream function, pressure gradient, and volume flow rate are derived. The relationship between flux and pressure difference is discussed. The effects of different pertinent parameters on variation of flux along the radius of the tube are analyzed through graphs. The results show that the yield stress and fluid behavior index has significant effect on flux variation of Herschel-Bulkley fluid in a non-uniform elastic tube. The effect of elastic parameters on flux variation is analyzed. Trapping phenomenon is presented graphically to understand the physical behavior of various parameters. In the absence of non-uniform parameter the present results are similar to the observations of Vajravelu et al. [19].

1. Introduction

Most of the earlier research works were concentrated on peristaltic pumping of non-Newtonian fluids through channels/tubes to understand the flow behavior of physiological fluids. The present study is modeled by considering the flow through a non-uniform elastic tube to describe the rheological characteristics of blood flow in a small blood vessel due to their elastic nature and non-uniform cross-section which has many practical biomedical applications. This non-uniform geometry is observed in the case of

*Corresponding author.
E-mail address: anssrinivas@vit.ac.in (A.N.S. Srinivas).
Peer review under responsibility of Beihang University.

Production and Hosting by Elsevier on behalf of KeAi

https://doi.org/10.1016/j.jppr.2018.07.010

Nomenclature

b	amplitude of the wave
ϕ	amplitude ratio
θ	azimuthal angle
a'	change in the radius of the tube due to peristalsis
a''	change in the radius of the tube due to elasticity
μ	coefficient of viscosity
τ_{rz}	shear stress
m	constant whose magnitude depends on length of the tube
σ	conductivity
z	distance along the tube from inlet end
ρ	density
q	dimensionless flux
t_1, t_2	elastic parameters
p_0	external pressure
p_1	inlet pressure
L	length of the tube
p_2	outlet pressure
n	power-law index
$p(z)$	pressure of the fluid
P	pressure gradient
a_0	radius of the tube in the absence of elasticity
$\dot{\gamma}$	shear rate
ψ	stream function
ψ_p	stream function in plug flow region
T	tension of the tube wall
t	time
u	velocity of the fluid flow
u_p	velocity of the plug flow
λ	wave length of the peristaltic wave
δ	wave number
c	wave speed
τ_0	yield stress

vasdeferens which is the part of male reproductive system. Although the geometric and kinematic properties of vasdeferens are not well established, it is generally observed to be a non-uniform duct. So study of mechanism of peristalsis in non-uniform geometry is used to understand the application of spermatic fluid flow in vasdeferens [1].

Herschel-Bulkley fluid is considered to understand the blood flow characteristics in small arteries. The effect of peristalsis and elasticity on non-Newtonian fluid flow in a tube of non-uniform cross section is examined. At low shear rates blood obeys the Casson fluid model that takes into account the yield stress of the fluid. By taking blood as a non-Newtonian fluid model, Scott Blair and Spanner [2] reported that blood obeys the Casson model for moderate shear rate flows. Further, the author observed, that, there is no difference between the Casson plots and Herschel-Bulkley plots of the experimental data over the range where the Casson plot is valid. It is observed that the Casson fluid model can be used for moderate shear rates in small diameter tubes whereas the Herschel-Bulkley fluid model can be used at still lower shear rate flow in very narrow arteries where the yield stress is high. Also the Herschel-Bulkley equation reduces to three different cases such as Bingham model, Power-law and Newtonian model for different conditions.

At first Latham [3] analyzed the motion of the fluid in the peristaltic pump experimentally. A detailed study on peristaltic motion in a channel and tubes for Newtonian fluid is made by Shapiro et al. [4] by taking long wavelengths and low Reynolds number approximations. The different types of Newtonian and non-Newtonian fluids are considered in the study of peristalsis to understand the behavior of physiological fluids. Rao and Mishra [5] discussed the peristaltic motion of power-law fluid in a porous tube. The influence of yield stress and amplitude ratio on peristaltic motion of Herschel-Bulkley fluid in a two dimensional channel is examined by Vajravelu et al. [6].

Further Vajravelu et al. [7] extended the study for inclined tube. Various researchers made theoretical and experimental investigations to understand the nature of peristaltic motion in different geometries under different assumptions. Nadeem and Akbar [8] discussed the Influence of heat transfer on a peristaltic transport of Herschel-Bulkley fluid in a non-uniform inclined tube.

The flow geometry plays an important role in understanding the nature of different fluid flows. Most of the earlier studies were concentrated on rigid channels and tubes. Some investigations on elastic nature of the tubes reveal many interesting behavior of arteries and small blood vessels since most of the vascular systems are flexible in nature. It is more adequate to consider such elastic nature of flow geometries to analyze the flow of physiological fluids. Roach and Burton [9] made an experimental study and presented the reason for the shape of distensibility curves of arteries. Whirlow and Rouleau [10] considered the viscous fluid flow in a thick walled elastic tube to understand nature of blood flow in arteries. Rubinow and Keller [11] discussed applications of blood flow by considering viscous fluid flow through elastic tube. Some earlier studies on elastic tubes were made by various researchers (Wang and Turbell [12], Misra and Ghosh [13], Sharma et al. [14], Pandey and Chaube [15]).

A mathematical model was proposed by Vajravelu et al. [16] to study the Herschel-Bulkley fluid flow in an elastic tube. Peristaltic pumping of viscous fluid in an elastic tube was investigated by Takagi and Balmforth [17]. The Newtonian and power-law fluids in elastic tubes are analyzed by Sochi [18]. Vajravelu et al. [19] discussed peristaltic transport of Herschel-Bulkley fluid in an elastic tube. Shen et al. [20] studied the conductivity of arterial pulsatile blood flow by an elastic model. Peristaltic transport of Casson fluid in an elastic tube is examined by Vajravelu et al. [21].

Impact of stratification and Cattaneo-Christov heat flux in the flow saturated with porous medium is studied by Nadeem and Muhammad [22]. Muhammad et al. [23] analyzed heat transport phenomenon in the ferro magnetic fluid over a stretching sheet with thermal stratification. Electro-osmotic flow of couple stress fluids in a micro

channel propagated by peristalsis is discussed by Tripathi et al. [24]. Tripathi et al. [25] investigated electro thermal transport of nanofluids via peristaltic pumping in a finite micro channel: effects of Joule heating and Helmholtz-Smoluchowski velocity. Nadeem et al. [26] studied mathematical analysis of ferromagnetic fluid embedded in a porous medium. Thermal radiation effects on electro osmosis modulated peristaltic transport of ionic nano liquids in biomicrofluidics channel is examined by Prakash et al. [27]. Three dimensional magnetohydrodynamic (MHD) flow of nanofluid over an exponential porous stretching sheet with convective boundary conditions is considered by Nayak et al. [28]. Muhammad et al. [29] analyzed the ferrite nano particles in the flow of ferromagnetic nanofluid.

Motivated by the above studies, a mathematical model is proposed to analyze the effect of elasticity on peristaltic transport of Herschel-Bulkley fluid in a non-uniform tube. The exact expressions for axial velocity, stream function and volume flow rate are obtained. The influence of different pertinent parameters on flux variation is analyzed through graphs.

2. Mathematical formulation

Figure 1 represents the peristaltic flow of incompressible Herschel-Bulkley fluid in a non-uniform elastic tube of length L and radius $a(z)$. The tube walls are subjected to infinite sinusoidal wave movement with constant speed c.

At any axial station z, the wall deformation of the tube is given by

$$\overline{r}=\overline{h}=\overline{a'}(\overline{z},\overline{t})=a_0+m\overline{z}+b\sin\left(\frac{2\pi}{\lambda}(\overline{z}-c\overline{t})\right) \tag{1}$$

The constitutive equation for Herschel-Bulkley fluid is

$$\tau=\mu(\dot{\gamma})^n+\tau_0 \text{ for } \tau\geq\tau_0,$$

$$\dot{\gamma}=0 \text{ for } \tau<\tau_0. \tag{2}$$

The equation of motion governing the flow is

$$\frac{1}{\overline{r}}\frac{\partial}{\partial\overline{r}}(\overline{r}\,\overline{\tau}_{rz})=-\frac{\partial\overline{p}}{\partial\overline{z}}, \tag{3}$$

Where

$$\overline{\tau}_{rz}=-\mu\left(\frac{\partial\overline{u}}{\partial\overline{r}}\right)^n+\overline{\tau}_0 \tag{4}$$

The appropriate boundary conditions are

$$\begin{aligned}&\overline{\tau}_{rz} \text{ is finite at } \overline{r}=0\\ &\overline{u}=0 \text{ at } \overline{r}=\overline{a'}(z,t)\end{aligned} \tag{5}$$

The non-dimensional quantities are

$$\begin{aligned}&r=\frac{\overline{r}}{a_0},\quad r=\frac{\overline{r}_0}{a_0},\quad z=\frac{\overline{z}}{\lambda},\quad u=\frac{\overline{u}}{c},\quad a'=\frac{\overline{a'}}{a_0},\quad a''=\frac{\overline{a''}}{a_0},\\ &t=\frac{c\overline{t}}{\lambda},\quad \phi=\frac{b}{a_0},\quad h=\frac{\overline{h}}{a_0},\quad p=\frac{a_0^{n+1}\overline{p}}{\lambda\mu c^n},\quad q=\frac{\overline{q}}{\pi a_0^2 c},\\ &\tau_0=\frac{\overline{\tau}_0}{\mu(c/a_0)^n},\quad \tau_{rz}=\frac{\overline{\tau}_{rz}}{\mu(c/a_0)^n},\quad \tau=\frac{\overline{\tau}}{\lambda\mu(c/a_0)^n}\\ &r=h=1+\frac{\lambda mz}{a_0}+\phi\sin2\pi(z-t)\end{aligned} \tag{6}$$

The governing equations in non-dimensional form are given by

$$\frac{1}{r}\frac{\partial}{\partial r}(r\tau_{rz})=P, \tag{7}$$

Where $P=-\frac{\partial p}{\partial z}$.

The non-dimensional boundary conditions are

$$\begin{aligned}&\tau_{rz} \text{ is finite at } r=0,\\ &u=0 \text{ at } r=h=a'(z,t).\end{aligned} \tag{8}$$

3. Solution of the problem

Solving Eq. (7) using the boundary condition (8), we get the velocity field as

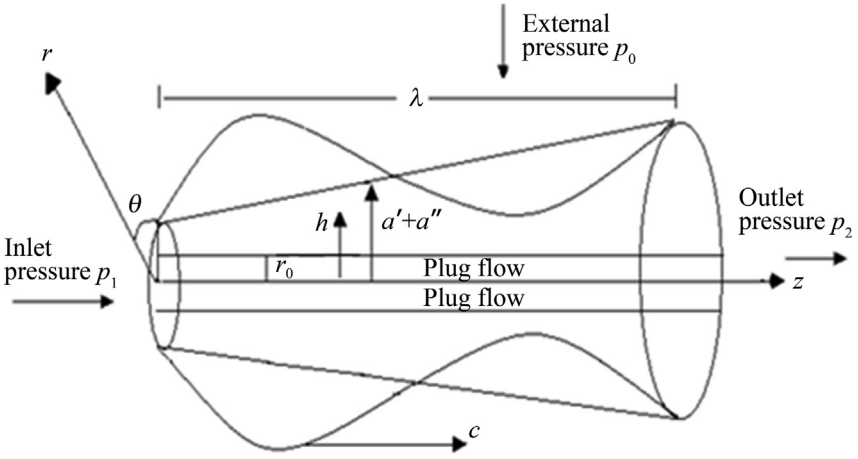

Figure 1 Physical model.

$$u=\frac{P^{\frac{1}{n}}}{2^{\frac{1}{n}}\left(\frac{1}{n}+1\right)}\left((a'-r_0)^{\frac{1}{n}+1}-(r-r_0)^{\frac{1}{n}+1}\right)\ \text{for}\ r_0\le r\le h. \tag{9}$$

using the boundary condition $\frac{\partial u}{\partial r}=0$ at $r=r_0$, The upper limit of the plug flow region is obtained as $r_0=2\tau_0/P$. Also using the condition $\tau_{rz}=\tau_{a'}$ at $r=a'$, we obtain $P=2\tau_{a'}/a'$. Hence

$$\frac{r_0}{a'}=\frac{\tau_0}{\tau_{a'}}=\tau\ \text{for}\ 0<\tau<1 \tag{10}$$

using the relation Eq. (10) and taking $r=r_0$ in Eq. (9), we get the plug flow velocity as

$$u_p=\frac{P^{\frac{1}{n}}}{2^{\frac{1}{n}}\left(\frac{1}{n}+1\right)}\left((a'-r_0)^{\frac{1}{n}+1}\right)\ \text{for}\ 0\le r\le r_0. \tag{11}$$

Integrating Eqs. (9) and (11) and using the conditions, $u=\frac{1}{r}\frac{\partial\psi}{\partial r}$, $\psi_p=0$ at $r=0$, and $\psi=\psi_p$ at $r=r_0$, we get the stream function as

$$\psi=\frac{P^{\frac{1}{n}}}{2^{\frac{1}{n}}\left(\frac{1}{n}+1\right)}\left[(h-r_0)^{\frac{1}{n}+1}\frac{r^2}{2}-\frac{(r-r_0)^{\frac{1}{n}+2}\left(2r+r\frac{1}{n}+r_0\right)}{\left(\frac{1}{n}+2\right)\left(\frac{1}{n}+3\right)}\right]\text{for}\ r_0\le r\le h. \tag{12}$$

and stream function for plug flow region as,

$$\psi_p=\frac{P^{\frac{1}{n}}a'^{\frac{1}{n}+1}}{2^k\left(\frac{1}{n}+1\right)}\left[(1-\tau_0)^{\frac{1}{n}+1}\right]\frac{r^2}{2}\ \text{for}\ 0\le r\le r_0. \tag{13}$$

The volume flux q through any cross-section is given by

$$q=2\int_0^{r_0}u_p r dr+2\int_0^{a'}u\,r dr=FP^{\frac{1}{n}}a'^{\frac{1}{n}+3}. \tag{14}$$

where $F=\frac{(1-\tau)^{\frac{1}{n}+1}}{2^{\frac{1}{n}}\left(\frac{1}{n}+1\right)}\left[1-\frac{2(1-\tau)\left(\tau+\frac{1}{n}+2\right)}{\left(\frac{1}{n}+2\right)\left(\frac{1}{n}+3\right)}\right]$.

The above Eq. (14) gives the volume flux of Herschel-Bulkley fluid for a non-uniform tube with peristalsis in the absence of elasticity.

4. Theoretical determination of flux application to blood flow through artery

In this section, the elasticity of the tube wall is taken in to consideration along with peristalsis to determine the variation of flux. Consider the peristaltic pumping of an incompressible Herschel-Bulkley fluid through a non-uniform elastic tube of radius $a(z)$ and length L as shown in Figure 1. Here $a(z)=a'+a''$ is the varying tube radius which consisting both peristalsis and elasticity effects. To calculate the flux of Herschel-Bulkley fluid through an elastic tube, we use the method of Rubinow and Keller [11]. Let p_1 and p_2 represents the pressure of fluid at the entrance and exit respectively and p_0 is the external pressure. Here the inlet pressure p_1 is assumed to be greater than outlet pressure p_2. As a result of inside and outside pressure difference, the tube wall may expand or contract. Due to this elastic property of the tube wall there exist changes in the shape of cross-section of tube. Hence, the conductivity σ of the tube at z depends on the pressure difference. Therefore the conductivity $\sigma=\sigma(p(z)-p_0)$ is a function of $(p(z)-p_0)$. Also, we assume that the flux q and the pressure gradient are related by the expression

$$q=\sigma(p-p_0)P^{\frac{1}{n}}. \tag{15}$$

From Eqs. (14) and (15), we have,

$$\sigma(p-p_0)=Fa'^{\frac{1}{n}+3}. \tag{16}$$

By taking elastic property into consideration in addition to the peristaltic movement, the above Eq. (16) can be written as

$$\sigma(p-p_0)=F(a'+a'')^{\frac{1}{n}+3}. \tag{17}$$

here a' and a'' are the radius of the tube with peristalsis and elasticity respectively. Since the flow is of Poiseuille type, the radius$a''$is a function of $(p-p_0)$ at each cross-section. The tube wall deformation due to peristaltic wave is

$$a'(z)=1+\frac{\lambda mz}{a_0}+\phi\sin 2\pi(z-t).$$

Integrating Eq. (15) with respect to z from the $z=0$ and applying inlet condition $p(0)=p_1$, we get

$$q^n z = \int_{p(z)-p_0}^{p_1-p_0} (\sigma(p'))^n dp'. \tag{18}$$

here $p' = p(z) - p_0$. The above Eq. (18) determines $p(z)$ implicitly in terms of q and z. To find Q we set $z=1$ and $p(1)=p_2$ in Eq. (18), which yields

$$q = F\left[\int_{p_2-p_0}^{p_1-p_0} (a'+a'')^{3n+1}\left[\frac{t_1}{a''^2}+t_2\left(4a''^3-15a''^2+20a''-10+\frac{1}{a''^2}\right)\right]da''\right]^{\frac{1}{n}} \tag{26}$$

$$q^n = \int_{p(1)-p_0}^{p_1-p_0} (\sigma(p'))^n dp' \tag{19}$$

using Eqs. (17) and (19), we have

$$q^n = F^n \int_{p_2-p_0}^{p_1-p_0} (a'+a'')^{3n+1} dp' \tag{20}$$

Eq. (20) can be solved if we know the form of the function $a''(p - p_0)$. If the stress or tension $T(a'')$ in the tube wall is known as a function of a'', then $a''(p')$ can be found using the equilibrium condition (Rubinow and Keller [11]).

$$T(a'')/a'' = p - p_0. \tag{21}$$

4.1. Method of Rubinow and Keller

Roach and Burton [9] determined the static pressure – volume relation experimentally by considering 4 cm long piece of the human external artery, and converted into a tension verses length curve. Using least squares method Rubinow and Keller [11], we have

$$T(a'') = t_1(a''-1) + t_2(a''-1)^5. \tag{22}$$

where $t_1 = 13$ and $t_2 = 300$, when we substitute Eq. (22) in Eq. (21), we get

$$p' = p - p_0 = \frac{1}{a''}\left[t_1(a''-1) + t_2(a''-1)^5\right]. \tag{23}$$

$$dp' = \left[\frac{t_1}{a''^2} + t_2\left(4a''^3 - 15a''^2 + 20a'' - 10 + \frac{1}{a''^2}\right)\right]da''. \tag{24}$$

Substituting Eq. (24) in Eq. (20), we get the flux as

$$q^n = F^n \int_{p_2-p_0}^{p_1-p_0} (a'+a'')^{3n+1}\left[\frac{t_1}{a''^2}+t_2\left(4a''^3-15a''^2+20a''-10+\frac{1}{a''^2}\right)\right]da'' \tag{25}$$

Rewriting Eq. (25), we have,

The Eq. (26) is difficult to evaluate and the fluid behavior index n takes the different values for both shear thinning and shear thickening cases. The experimental works presented in Table 1 on shear thinning fluids like apple sauce and banana puree at different temperatures shows that, in particular the power-law index value is taken as $n = 1/3$ (Cheremisinoff [30]).

Solving Eq. (26) with $n = 1/3$ we get,

$$q = F[g(a''_1) - g(a''_2)]^3 \tag{27}$$

where

$$g(a) = t_1\left(a'' + 2a'\log a'' - a'^2/a''\right) + t_2\left(\begin{array}{l} 2a''^6/3 + a''^5/5(8a'-15) + a''^4/4(4a'^2-30a'+20) \\ + a''^3/3(-15a'^2+40a'-10) + a''^2/2(20a'^2-20a') \\ + a''(-10a'^2+1) - \dfrac{a'^2}{a''} + 2a'\log a'' \end{array}\right)a'' \tag{28}$$

5. Results and discussion

Peristaltic transport of Herschel-Bulkley fluid in a non-uniform elastic tube is investigated in the present paper. The

Table 1 Values of m and n for banana puree and apple sauce at different temperatures.

Fluid	Temperature	Category	m	n
Banana puree	168	Shear thinning	68.9	0.46
	120	Shear thinning	41.5	0.48
Apple sauce	77	Shear thinning	220	0.28

influence of various parameters such as amplitude ratio ϕ, yield stress τ_0, power-law index n, elastic parameters t_1 and t_2, inlet and outlet pressure on flux variation along non-uniform tube radius using Rubinow and Keller method is analyzed through graphs.

The variation of flux along non-uniform tube radius for different values of yield stress τ_0, amplitude ratio ϕ, power-law index n, inlet pressure and outlet pressure are shown in Figures 2—7 respectively. It is noticed from Figure 2 that the increasing values of yield stress parameter has significant effect on volume flow rate of Herschel-Bulkley fluid. That is the flux decreases as yield stress increases because the increasing yield stress increases the resistance to flow hence the velocity of the fluid gets reduced which yields to decrease in the flux. The influence of amplitude ratio on flux variation is illustrated in Figure 3. It is clear that the flux enhances for increasing values of ϕ. That is increasing amplitude ratio enhances the maximum displacement of the fluid particles. The flux variation for different values of fluid behavior index n for both shear thinning and shear

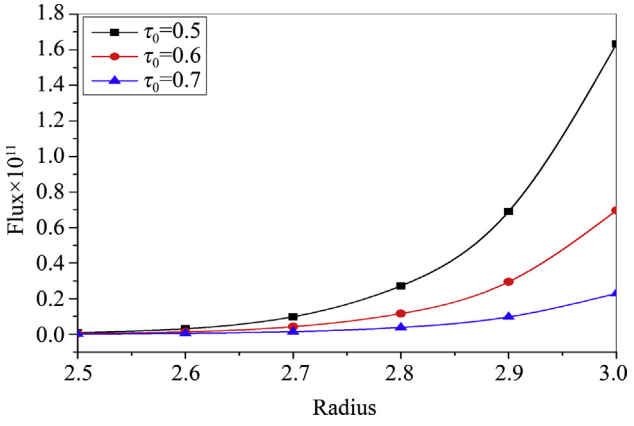

Figure 2 Flux vs. radius for different values of yield stress τ_0 with $t_1=13$, $t_2=300$, $z=0.1$, $\phi=0.6$, $a_0=0.01$, $m=0.0005$, $\lambda=1$, $n=0.333$, $t=0.01$.

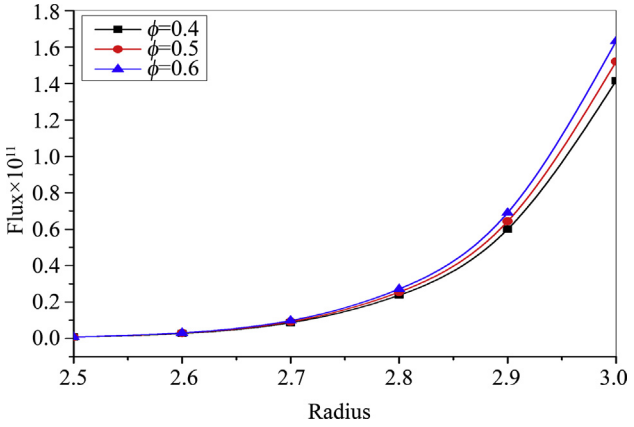

Figure 3 Flux vs. radius for different values of amplitude ratio ϕ with $t_1=13$, $t_2=300$, $z=0.1$, $\tau_0=0.5$, $a_0=0.01$, $m=0.0005$, $\lambda=1$, $n=0.333$, $t=0.01$.

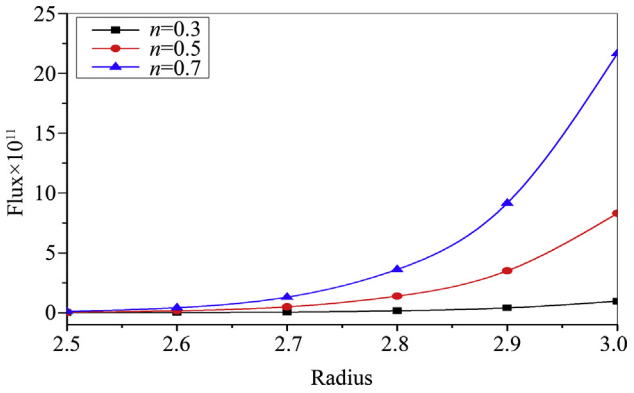

Figure 4 Flux vs. radius for different values of power-law index n with $t_1=13$, $t_2=300$, $z=0.1$, $\phi=0.6$, $a_0=0.01$, $m=0.0005$, $\lambda=1$, $\tau_0=0.5$, $t=0.01$ (for shear thinning fluid).

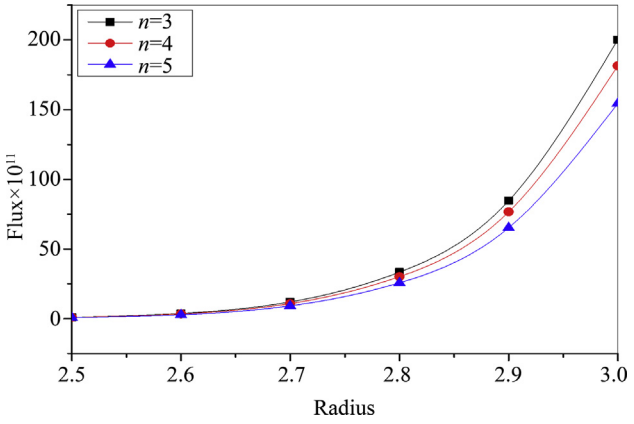

Figure 5 Flux vs. radius for different values of power-law index n with $t_1=13$, $t_2=300$, $z=0.1$, $\tau_0=0.5$, $a_0=0.01$, $m=0.0005$, $\lambda=1$, $\phi=0.6$, $t=0.01$ (for shear thickening fluid).

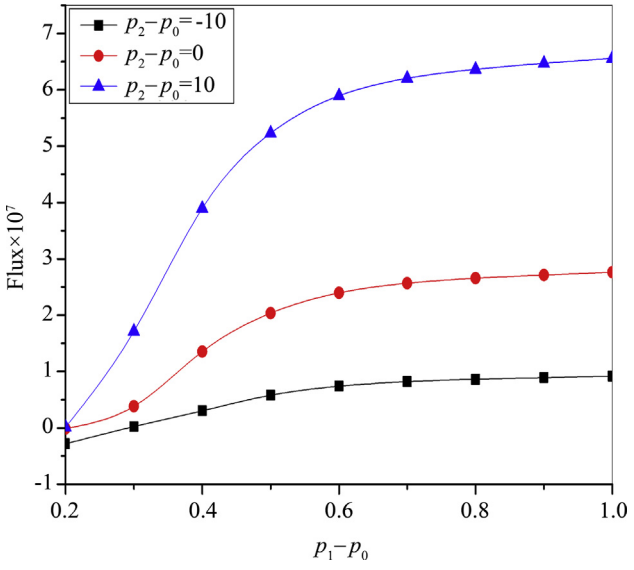

Figure 6 Flux vs. inlet pressure for different values of outlet pressure with $t_1=13$, $t_2=300$, $z=0.1$, $\phi=0.6$, $a_0=0.01$, $m=0.0005$, $\lambda=1$, $\tau_0=0.1$, $n=0.333$, $t=0.01$.

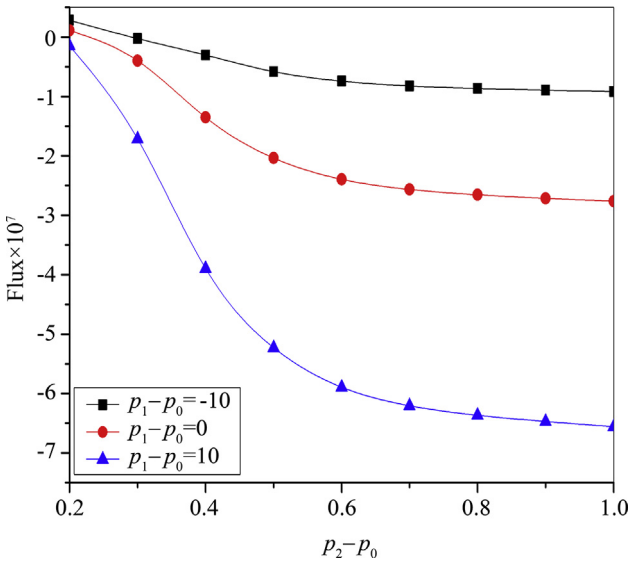

Figure 7 Flux vs. outlet pressure for different values of inlet pressure with $t_1 = 13$, $t_2 = 300$, $z = 0.1$, $\phi = 0.6$, $a_0 = 0.01$, $m = 0.0005$, $\lambda = 1$, $\tau_0 = 0.1$, $n = 0.333$, $t = 0.01$.

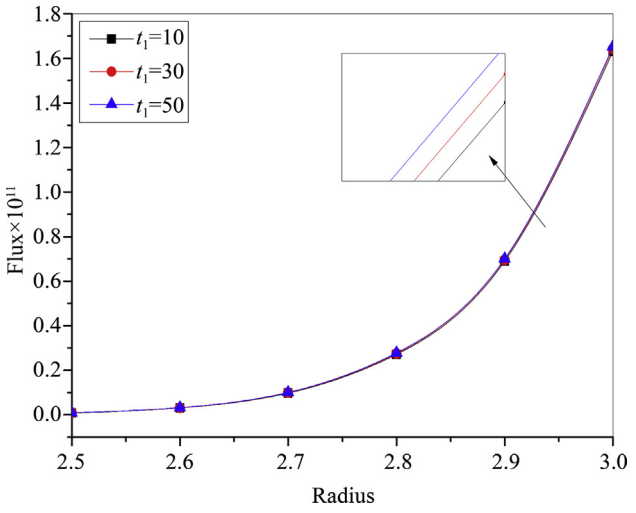

Figure 8 Flux vs. radius for different values of elastic parameter t_1 with $t_2 = 300$, $z = 0.1$, $\phi = 0.6$, $a_0 = 0.01$, $m = 0.0005$, $\lambda = 1$, $\tau_0 = 0.1$, $n = 0.333$, $t = 0.01$.

thickening fluids are shown in Figures 4 and 5 respectively. It is found from Figure 4 that increasing n for shear thinning fluids enhances the flux. In shear thinning fluids viscosity decreases with increasing shear rate, hence the resistance to flow decreases. Therefore the fluid velocity increases which increases the flux. The opposite trend is observed for shear thickening case in Figure 5.

Figure 6 represents the variation in flux along inlet pressure and external pressure difference $p_1 - p_0$ for different values of outlet and external pressure difference $p_2 - p_0$. It is observed that the flux increases with increasing values of $p_2 - p_0$ due to non-uniform pressure difference at inlet and outlet pressure. The opposite behavior is observed in the case of inlet pressure and external pressure difference $p_1 - p_0$. That is from Figure 7 it is noticed that the flux reduces with increasing values of $p_1 - p_0$ for fixed values outlet and external pressure difference $p_2 - p_0$. The flux variation along non-uniform elastic tube for different values of elastic parameters t_1 and t_2 are presented in Figures 8 and 9 respectively. The results reveal that the flux enhances with increasing values of elastic parameters t_1 and t_2. That is increasing elastic parameter increases the flexible nature of the tube. So the cross-section of the tube increases which enhances the flux.

Trapping is another interesting phenomenon observed in peristalsis mechanism. The effects of different pertinent parameters power-law index n, yield stress τ_0, amplitude ratio ϕ and elastic radius parameter a'' on the size of trapped bolus are presented in Figures 10–14 respectively. Figures 10 and 11 represent the effect of power-law index n on bolus size for both shear thinning and thickening fluids. It is noticed that the bolus size decreases with increasing values of fluid behavior index.

Figure 12 illustrates that the size of the trapped bolus reduces with increasing values of yield stress parameter τ_0. The influence of amplitude ratio ϕ on the bolus is illustrated in Figure 13. It is clear that the bolus size enhances with increasing values of ϕ. The effect of elasticity parameter on trapping is observed from Figure 14 and it is clear that the bolus size enhances as a'' increases. Figure 15 represents the variation in the flux for different values of yield stress τ_0 in the absence of non-uniform parameter. It is observed that if $m = 0$, the present results are similar to the observations of Vajravelu et al. [19].

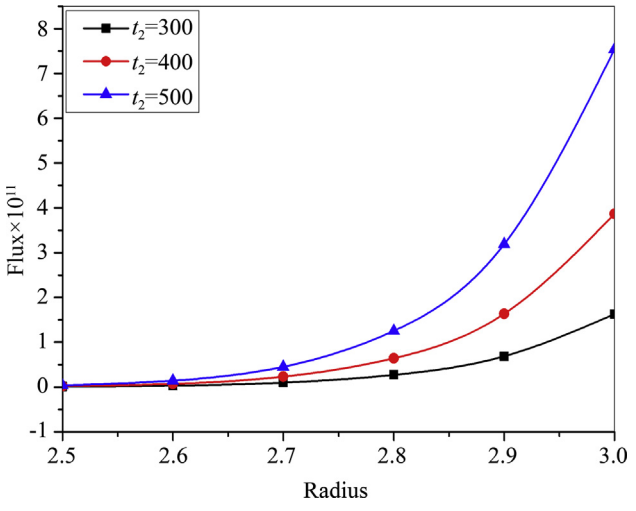

Figure 9 Flux vs. radius for different values of elastic parameter t_2 with $t_1 = 13$, $z = 0.1$, $\phi = 0.6$, $a_0 = 0.01$, $m = 0.0005$, $\lambda = 1$, $\tau_0 = 0.1$, $n = 0.333$, $t = 0.01$.

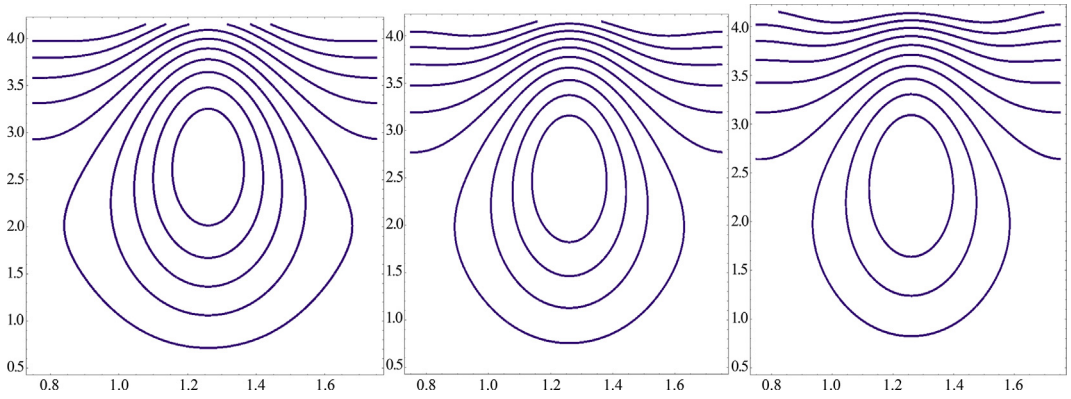

Figure 10 Streamlines with $m = 0.005$, $\lambda = 0.1$, $a_0 = 1$, $\phi = 0.2$, $Q = 0.5$, $\tau = 0.1$, $a'' = 0.3$, $t = 0.01$ and (i) $n = 10$ (ii) $n = 20$ (iii) $n = 30$ (for shear thickening fluids).

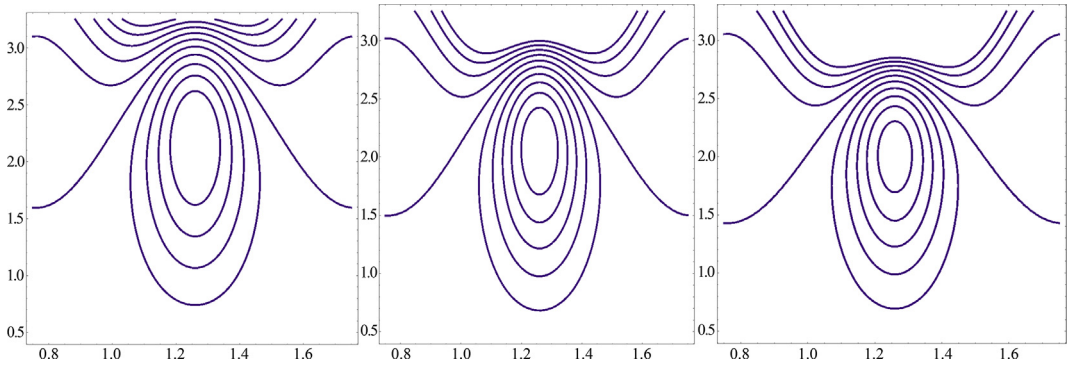

Figure 11 Streamlines with $m = 0.005$, $\lambda = 0.1$, $a_0 = 1$, $\phi = 0.2$, $Q = 0.5$, $\tau = 0.1$, $a'' = 0.3$, $t = 0.01$ and (i) $n = 0.2$ (ii) $n = 0.3$ (iii) $n = 0.4$ (for shear thinning fluids).

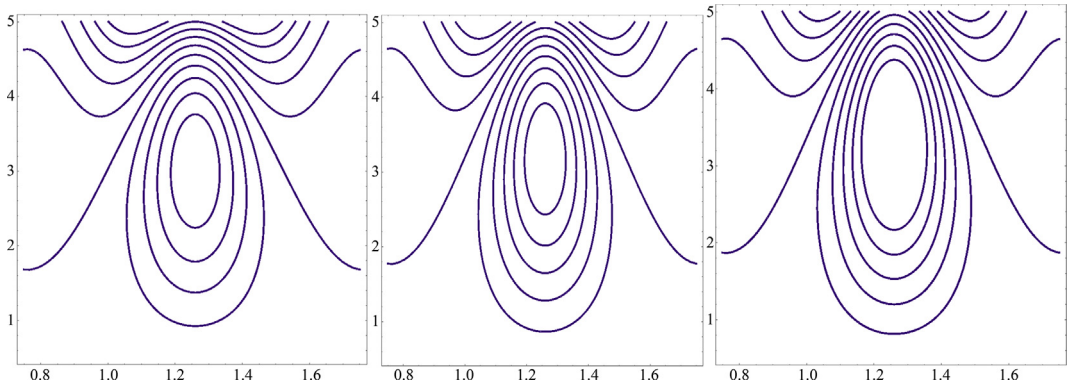

Figure 12 Streamlines with $m = 0.005$, $\lambda = 0.1$, $a_0 = 1$, $\phi = 0.2$, $Q = 0.5$, $n = 0.333$, $a'' = 0.3$, $t = 0.01$ and (i) $\tau_0 = 0.3$ (ii) $\tau_0 = 0.4$ (iii) $\tau_0 = 0.5$.

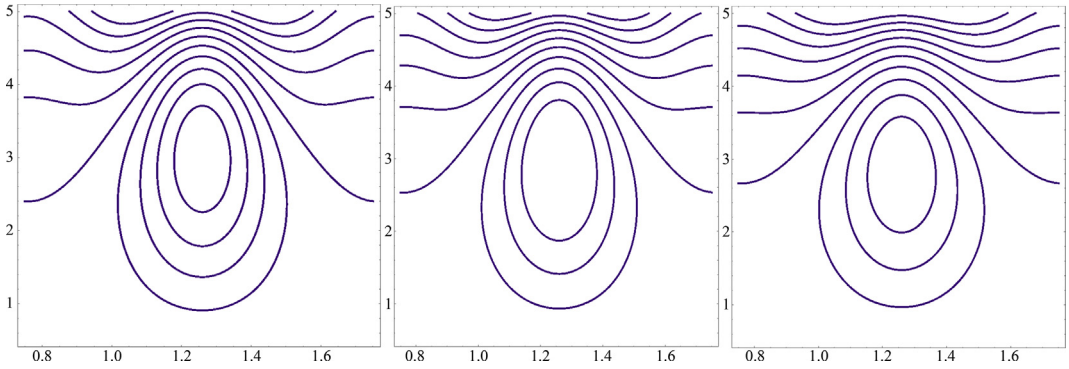

Figure 13 Streamlines with $m=0.005$, $\lambda=0.1$, $a_0=1$, $n=0.333$, $Q=0.5$, $\tau=0.1$, $a''=0.3$, $t=0.01$ and (i) $\phi = 0.3$ (ii) $\phi = 0.4$ (iii) $\phi = 0.5$.

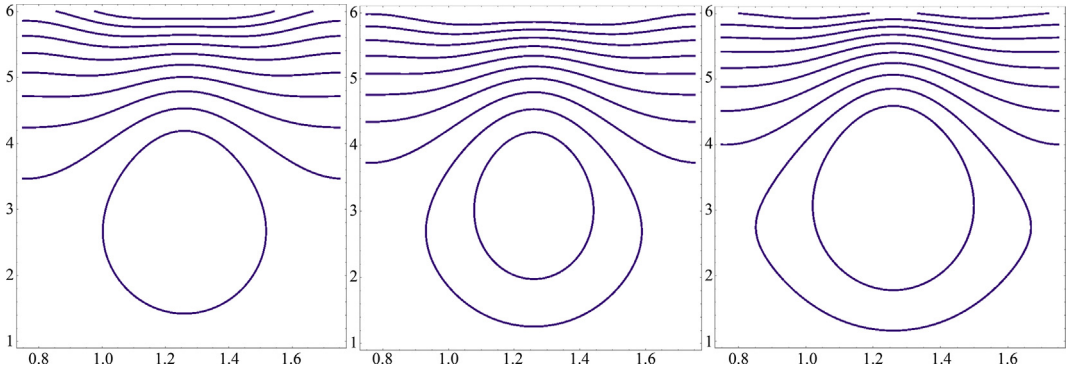

Figure 14 Streamlines with $m=0.005$, $\lambda=0.1$, $a_0=1$, $n=0.333$, $Q=0.5$, $\tau_0=0.1$, $\phi=0.2$, $t=0.01$ and (i) $a''=0.5$ (ii) $a''=0.6$ (iii) $a''=0.7$.

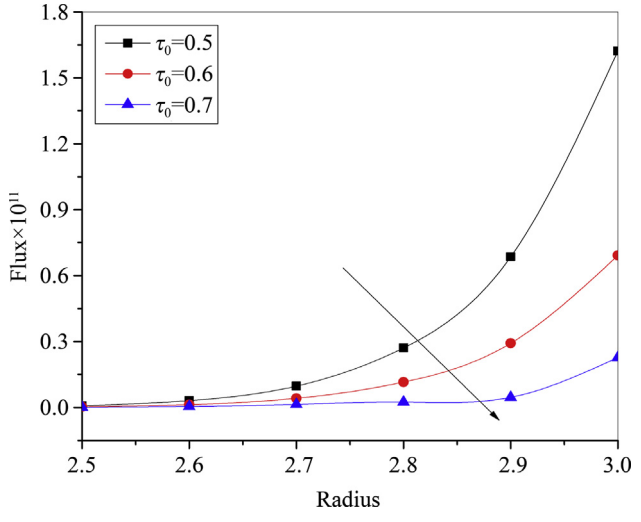

Figure 15 Flux vs. radius for different values of yield stress τ_0 in the absence of non-uniform parameter $(m=0)$ with $t_1=13$, $t_2=300$, $z=0.1$, $\phi=0.6$, $n=0.333$, $t=0.01$, $a'=1+\phi\sin 2\pi(z-t)$ (Vajravelu at al [19]).

6. Conclusions

The present study deals with the peristaltic transport of a Herschel-Bulkley fluid in a non-uniform elastic tube. The analytic expressions for axial velocity, volume flow rate and stream function are presented. The effects of various physical parameters on volume flow rate are calculated by Rubinow and Keller method [11]. The trapping phenomenon is explained graphically. The important observations are summarized as follows.

i) The flux as a function of non-uniform tube radius increases for increasing values of amplitude ratio ϕ and it decreases for yield stress parameter τ_0
ii) The flux of Herschel-Bulkley fluid in a non-uniform tube with peristalsis and elasticity decreases as fluid behavior index$n$ (for both shear thinning$(n<1)$ and shear thickening$(n>1)$) increases.
iii) The flux as a function of inlet pressure increases as outlet pressure increases but the opposite behavior is observed for the case of increasing values of inlet pressure.

iv) The variation in flux enhances with growing values of elastic parameters t_1 and t_2.
v) The size of the trapped bolus increases for increasing values of ϕ and a'' and it decreases as τ_0 and n increases.

Acknowledgement

The authors thank the referees for their constructive comments which lead to betterment of the article.

References

[1] B.B. Gupta, V. Seshadri, Peristaltic pumping in non-uniform tubes, J. Biomech. 9 (1976) 105−109.
[2] G.W.S. Blair, D.C. Spanner, An Introduction to Bioreheology, Elsevier, Amsterdam, 1974.
[3] T.W. Latham, Fluid motions in a peristaltic pump, MS Thesis, Massachusetts Institute of Technology, Cambridge, 1966.
[4] A.H. Shapiro, M.Y. Jaffrin, S.L. Weinberg, Peristaltic pumping with long wavelengths at low Reynolds number, J. Fluid Mech. 37 (1969) 799−825.
[5] A.R. Rao, M. Mishra, Peristaltic transport of a power-law fluid in a porous tube, J. Non-Newtonian Fluid Mech. 121 (2004) 163−174.
[6] K. Vajravelu, S. Sreenadh, V. Ramesh Babu, Peristaltic pumping of Herschel-Bulkley fluid in a channel, Appl. Math. Comput. 169 (2005) 726−735.
[7] K. Vajravelu, S. Sreenadh, V. Ramesh Babu, Peristaltic transport of a Herschel-Bulkley fluid in an inclined tube, Int. J. Non-Linear Mech. 40 (2005) 83−90.
[8] S. Nadeem, N.S. Akbar, Influence of heat transfer on a peristaltic transport of Herschel-Bulkley fluid in a non uniform inclined tube, Commun. Nonlinear Sci. Numer. Simul. 14 (2009) 4100−4113.
[9] M.R. Roach, A.C. Burton, The reason for the shape of distensibility curves of arteries, Can. J. Biochem. Physiol. 35 (1957) 681−690.
[10] D.K. Whirlow, W.T. Rouleau, Periodic flow of a viscous fluid in a thick-walled elastic tube, Bull. Math. Biophys. 27 (1965) 355−370.
[11] S.L. Rubinow, J.B. Keller, Flow of a viscous fluid through an elastic tube with applications to blood flow, J. Theor. Biol. 35 (1972) 299−313.
[12] D.M. Wang, J.M. Tarbell, Non linear analysis of flow in an elastic tube (artery): steady streaming effects, J. Fluid Mech. 239 (1992) 341−358.
[13] J.C. Misra, S.K. Ghosh, Pulsatile flow of a viscous fluid through a porous elastic vessel of variable cross-section − a mathematical model for hemodynamic flows, Comput. Math. Appl. 46 (2003) 947−957.
[14] G.C. Sharma, M. Jain, A. Kumar, Performance modeling and analysis of blood flow in elastic arteries, Mathematical and Computer Modeling 39 (2004) 1491−1499.
[15] S.K. Pandey, M.K. Chaube, Peristaltic transport of a visco-elastic fluid in a tube of a non-uniform cross-section, Mathematical and Computer Modeling 52 (2010) 501−514.
[16] K. Vajravelu, S. Sreenadh, P. Devaki, K.V. Prasad, Mathematical model for a Herschel-Bulkley fluid flow in an elastic tube, Cent. Eur. J. Phys. 9 (2011) 1357−1365.
[17] D. Takagi, N.J. Balmforth, Peristaltic pumping of viscous fluid in an elastic tube, J. Fluid Mech. 672 (2011) 196−218.
[18] T. Sochi, The flow of Newtonian and power-law fluids in elastic tubes, Int. J. Non-Linear Mech. 67 (2014) 245−250.
[19] K. Vajravelu, S. Sreenadh, P. Devaki, K.V. Prasad, Peristaltic transport of a Herschel-Bulkley fluid in an elastic tube, Heat Transf. Asian Res. 44 (2014) 585−598.
[20] H. Shen, Y. Zhu, K.R. Qin, A theoretical computerized study for the electrical conductivity of arterial pulsatile blood flow by an elastic tube model, Med. Eng. Phys. 38 (2016) 1439−1448.
[21] K. Vajravelu, S. Sreenadh, P. Devaki, K.V. Prasad, Peristaltic pumping of a Casson fluid in an elastic tube, J. Appl. Fluid Mech. 9 (2016) 1897−1905.
[22] S. Nadeem, N. Muhammad, Impact of stratification and Cattaneo-christov heat flux in the flow saturated with porous medium, J. Mol. Liq. 224 (2016) 423−430.
[23] N. Muhammad, S. Nadeem, R. UI Haq, Heat transport phenomenon in the ferro magnetic fluid over a stretching sheet with thermal stratification, Results in Physics 7 (2017) 854−861.
[24] D. Tripathi, A. Yadav, O.A. Bég, Electro-osmotic flow of couple stress fluids in a micro channel propagated by peristalsis, The European Physical Journal Plus 132 (2017) 173.
[25] D. Tripathi, A. Sharma, O.A. Bég, Electro thermal transport of nanofluids via peristaltic pumping in a finite micro channel: effects of Joule heating and Helmholtz-Smoluchowski velocity, Int. J. Heat Mass Transf. 111 (2017) 138−149.
[26] S. Nadeem, I. Raishad, N. Muhammad, M.T. Mustafa, Mathematical analysis of ferromagnetic fluid embedded in a porous medium, Results in Physics 7 (2017) 2361−2368.
[27] J. Prakash, A. Sharma, D. Tripathi, Thermal radiation effects on electro osmosis modulated peristaltic transport of ionic nano liquids in biomicrofluidics channel, J. Mol. Liq. 249 (2018) 843−855.
[28] M.K. Nayak, N.S. Akbar, D. Tripathi, V.S. Pandey, Three dimensional MHD flow of nanofluid over an exponential porous stretching sheet with convective boundary conditions, Thermal Science and Engineering Progress 3 (2017) 133−140.
[29] N. Muhammad, S. Nadeem, M.T. Mustafa, Analysis of ferrite nanoparticles in the flow of ferromagnetic nanofluid, PLAS One 13 (2018) pmc5761848.
[30] N.P. Cheremisinoff, Encyclopedia of Fluid Mechanics, Rheology of Non-Newtonian Flows, Gulf Publishing Co., Houston, TX, 1988.